

Graph Drawing via Gradient Descent, $(GD)^2$

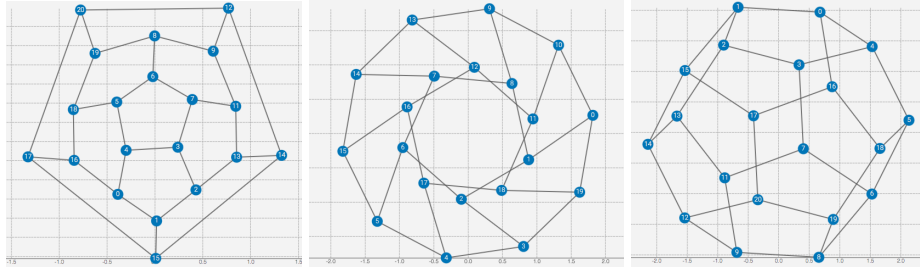
Reyan Ahmed, Felice De Luca, Sabin Devkota, Stephen Kobourov, Mingwei Li

Department of Computer Science, University of Arizona, USA

1 **Abstract.** Readability criteria, such as distance or neighborhood preser-
2 vation, are often used to optimize node-link representations of graphs to
3 enable the comprehension of the underlying data. With few exceptions,
4 graph drawing algorithms typically optimize one such criterion, usually
5 at the expense of others. We propose a layout approach, Graph Drawing
6 via Gradient Descent, $(GD)^2$, that can handle multiple readability crite-
7 ria. $(GD)^2$ can optimize any criterion that can be described by a smooth
8 function. If the criterion cannot be captured by a smooth function, a
9 non-smooth function for the criterion is combined with another smooth
10 function, or auto-differentiation tools are used for the optimization. Our
11 approach is flexible and can be used to optimize several criteria that
12 have already been considered earlier (e.g., obtaining ideal edge lengths,
13 stress, neighborhood preservation) as well as other criteria which have
14 not yet been explicitly optimized in such fashion (e.g., vertex resolution,
15 angular resolution, aspect ratio). We provide quantitative and qualitative
16 evidence of the effectiveness of $(GD)^2$ with experimental data and a func-
17 tional prototype: <http://hdc.cs.arizona.edu/~mwli/graph-drawing/>.

18 1 Introduction

19 Graphs represent relationships between entities and visualization of this infor-
20 mation is relevant in many domains. Several criteria have been proposed to eval-
21 uate the readability of graph drawings, including the number of edge crossings,
22 distance preservation, and neighborhood preservation. Such criteria evaluate dif-
23 ferent aspects of the drawing and different layout algorithms optimize different
24 criteria. It is challenging to optimize multiple readability criteria at once and
25 there are few approaches that can support this. Examples of approaches that
26 can handle a small number of related criteria include the stress majorization
27 framework of Wang et al. [34], which optimizes distance preservation via stress
28 as well as ideal edge length preservation. The Stress Plus X (SPX) framework
29 of Devkota et al. [12] can minimize the number of crossings, or maximize the
30 minimum angle of edge crossings. While these frameworks can handle a limited
31 set of related criteria, it is not clear how to extend them to arbitrary optimiza-
32 tion goals. The reason for this limitation is that these frameworks are dependent
33 on a particular mathematical formulation. For example, the SPX framework was
34 designed for crossing minimization, which can be easily modified to handle cross-
35 ing angle maximization (by adding a cosine factor to the optimization function).
36 This “trick” can be applied only to a limited set of criteria but not the majority
37 of other criteria that are incompatible with the basic formulation.



38 **Fig. 1.** Three $(GD)^2$ layouts of the dodecahedron: (a) optimizing the number of
 39 crossings, (b) optimizing uniform edge lengths, and (c) optimizing stress.

40 In this paper, we propose a general approach, Graph Drawing via Gradient
 41 Descent, $(GD)^2$, that can optimize a large set of drawing criteria, provided that
 42 the corresponding metrics that evaluate the criteria are smooth functions. If the
 43 function is not smooth, $(GD)^2$ either combines it with another smooth function
 44 and partially optimizes based on the desired criterion, or uses modern auto-
 45 differentiation tools to optimize. As a result, the proposed $(GD)^2$ framework
 46 is simple: it only requires a function that captures a desired drawing criterion.
 47 To demonstrate the flexibility of the approach, we consider an initial set of
 48 nine criteria: minimizing stress, maximizing vertex resolution, obtaining ideal
 49 edge lengths, maximizing neighborhood preservation, maximizing crossing angle,
 50 optimizing total angular resolution, minimizing aspect ratio, optimizing the
 51 Gabriel graph property, and minimizing edge crossings. A functional prototype
 52 is available on <http://hdc.cs.arizona.edu/~mwli/graph-drawing/>. This is
 53 an interactive system that allows vertices to be moved manually. Combinations
 54 of criteria can be optimized by selecting a weight for each; see Figure 1.

55 2 Related Work

56 Many criteria associated with the readability of graph drawings have been pro-
 57 posed [35]. Most of graph layout algorithms are designed to (explicitly or implic-
 58 itly) optimize a single criterion. For instance, a classic layout criterion is stress
 59 minimization [24], where stress is defined by $\sum_{i < j} w_{ij} (|X_i - X_j| - d_{ij})^2$. Here, X is
 60 a $n \times 2$ matrix containing coordinates for the n nodes, d_{ij} is typically the graph-
 61 theoretical distance between two nodes i and j and $w_{ij} = d_{ij}^{-\alpha}$ is a normalization
 62 factor with α equal to 0, 1 or 2. Thus reducing the stress in a layout corresponds
 63 to computing node positions so that the actual distance between pairs of nodes
 64 is proportional to the graph theoretic distance between them. Optimizing stress
 65 can be accomplished by stress minimization, or stress majorization, which can
 66 speed up the computation [20]. In this paper we only consider drawing in the
 67 Euclidean plane, however, stress can be also optimized in other spaces such as
 68 the torus [8].

69 Stress minimization corresponds to optimizing the global structure of the
70 layout, as the stress metric takes into account all pairwise distances in the graph.
71 The t-SNET algorithm of Krueger et al. [25] directly optimizes neighborhood
72 preservation, which captures the local structure of a graph, as the neighborhood
73 preservation metric only considers distances between pairs of nodes that are close
74 to each other. Optimizing local or global distance preservation can be seen as
75 special cases of the more general dimensionality reduction approaches such as
76 multi-dimensional scaling [26, 32].

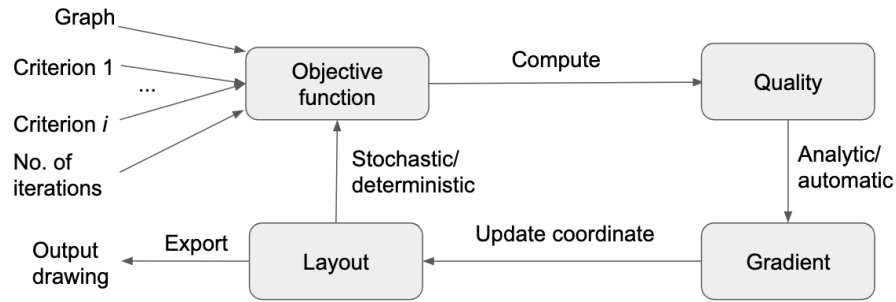
77 Purchase et al. [28] showed that the readability of graphs increases if a lay-
78 out has fewer edge crossings. The underlying optimization problem is NP-hard
79 and several graph drawing contests have been organized with the objective of
80 minimizing the number of crossings in the graph drawings [2, 7]. Recently several
81 algorithms that directly minimize crossings have been proposed [29, 31].

82 The negative impact on graph readability due to edge crossings can be miti-
83 gated if crossing pairs of edges have a large crossings angle [3, 13, 22, 23]. Formally,
84 the crossing angle of a straight-line drawing of a graph is the minimum angle
85 between two crossing edges in the layout, and optimizing this property is also
86 NP-hard. Recent graph drawing contests have been organized with the objective
87 of maximizing the crossings angle in graph drawings and this has led to several
88 heuristics for this problem [4, 10].

89 The algorithms above are very effective at optimizing the specific readability
90 criterion they are designed for, but they cannot be directly used to optimize
91 additional criteria. This is a desirable goal, since optimizing one criterion often
92 leads to poor layouts with respect to one or more other criteria: for example,
93 algorithms that optimize the crossing angle tend to create drawings with high
94 stress and no neighborhood preservation [12].

95 Recently, several approaches have been proposed to simultaneously improve
96 multiple layout criteria. Wang et al. [34] propose a revised formulation of stress
97 that can be used to specify ideal edge direction in addition to ideal edge lengths
98 in a graph drawing. Devkota et al. [12] also use a stress-based approach to min-
99 imize edge crossings and maximize crossing angles. Eades et al. [17] provided a
100 technique to draw large graphs while optimizing different geometric criteria, in-
101 cluding the Gabriel graph property. Although the approaches above are designed
102 to optimize multiple criteria, they cannot be naturally extended to handle other
103 optimization goals.

104 Constraint-based layout algorithms such as COLA [15, 16], can be used to
105 enforce separation constraints on pairs of nodes to support properties such as
106 customized node ordering or downward pointing edges. The coordinates of two
107 nodes are related by inequalities in the form of $x_i \geq x_j + gap$ for a node pair
108 (i, j) . These kinds of constraints are known as hard constraints and are different
109 from the soft constrains in our $(GD)^2$ framework.



128 **Fig. 2.** The $(GD)^2$ framework: Given a graph and a set of criteria (with weights),
 129 formulate an objective function based on the selected set of criteria and weights.
 130 Then compute the quality (value) of the objective function of the current layout
 131 of the graph. Next, generate the gradient (analytically or automatically). Using
 132 the gradient information, update the coordinates of the layout. Finally, update
 133 the objective function based on the layout via regular or stochastic gradient
 134 descent. This process is repeated for a fixed number of iterations.

110 3 The $(GD)^2$ Framework

111 The $(GD)^2$ framework is a general optimization approach to generate a layout
 112 with any desired set of aesthetic metrics, provided that they can be expressed by
 113 a smooth function. The basic principles underlying this framework are simple.
 114 The first step is to select a set of layout readability criteria and a loss functions
 115 that measures them. Then we define the function to optimize as a linear combi-
 116 nation of the loss functions for each individual criterion. Finally, we iterate the
 117 gradient descent steps, from which we obtain a slightly better drawing at each
 118 iteration. Figure 2 depicts the framework of $(GD)^2$: Given any graph G and read-
 119 ability criterion Q , we find a loss function $L_{Q,G}$ which maps from the current
 120 layout X (i.e. a $n \times 2$ matrix containing the positions of nodes in the draw-
 121 ing) to a real value that quantifies the current drawing. Note that some of the
 122 readability criteria naturally correspond to functions that should be minimized
 123 (e.g., stress, crossings), while others to functions that should be maximized (e.g.,
 124 neighborhood preservation, angular resolution). Given a loss function $L_{Q,G}$ of X
 125 where a lower value is always desirable, at each iteration, a slightly better layout
 126 can be found by taking a small (ϵ) step along the (negative) gradient direction:
 127 $X^{(new)} = X - \epsilon \cdot \nabla_X L_{Q,G}$.

135 To optimize multiple quality measures simultaneously, we take a weighted
 136 sum of their loss functions and update the layout by the gradient of the sum.

137 3.1 Gradient Descent Optimization

138 There are different kinds of gradient descent algorithms. The standard method
 139 considers all vertices, computes the gradient of the objective function, and up-
 140 dates vertex coordinates based on the gradient. For some objectives, we need

141 to consider all the vertices in every step. For example, the basic stress formu-
 142 lation [24] falls in this category. On the other hand, there are some problems
 143 where the objective can be optimized only using a subset of vertices. For exam-
 144 ple, consider stress minimization again. If we select a set of vertices randomly
 145 and minimize the stress of the induced graph, the stress of the whole graph is
 146 also minimized [36]. This type of gradient descent is called stochastic gradient
 147 descent. However, not all objective functions are smooth and we cannot compute
 148 the gradient of a non-smooth function. In that scenario, we can compute the sub-
 149 gradient, and update the objective based on the subgradient. Hence, as long as
 150 the function is continuously defined on a connected component in the domain,
 151 we can apply the subgradient descent algorithm. In table 3, we give a list of loss
 152 functions we used to optimize 9 graph drawing properties with gradient descent
 153 variants. In section 4, we specify the loss functions we used in detail.

154 When a function is not defined in a connected domain, we can introduce a
 155 surrogate loss function to ‘connect the pieces’. For example, when optimizing
 156 neighborhood preservation we maximize the Jaccard similarity between graph
 157 neighbors and nearest neighbors in graph layout. However, Jaccard similarity
 158 is only defined between two binary vectors. To solve this problem we extend
 159 Jaccard similarity to all real vectors by its Lovász extension [5] and apply that to
 160 optimize neighborhood preservation. An essential part of gradient descent based
 161 algorithms is to compute the gradient/subgradient of the objective function. In
 162 practice, it is always not necessary to write down the gradient analytically as it
 163 can be computed automatically via automatic differentiation [21]. Deep learning
 164 packages such as Tensorflow [1] and PyTorch [27] apply automatic differentiation
 165 to compute the gradient of complicated functions.

166 When optimizing multiple criteria simultaneously, we combine them via a
 167 weighted sum. However, choosing a proper weight for each criterion can be tricky.
 168 Consider, for example, maximizing crossing angles and minimize stress simulta-
 169 neously with a fixed pair of weights. At the very early stage, the initial drawing
 170 may have many crossings and stress minimization often removes most of the
 171 early crossings. As a result, maximizing crossing angles in those early stages can
 172 be harmful as moves nodes in direction that contradict those that come from
 173 stress minimization. Therefore, a well-tailored *weight scheduling* is needed for a
 174 successful outcome. Continuing with the same example, a better outcome can be
 175 achieved by first optimizing stress until it converges, and later adding weights
 176 for the crossing angle maximization. To explore different ways of scheduling, we
 177 provide an interface that allows manual tuning of the weights.

178 3.2 Implementation

179 We implemented the $(GD)^2$ framework in JavaScript. In particular we used
 180 the automatic differentiation tools in tensorflow.js [33] and the drawing library
 181 d3.js [6]. The prototype is available at <http://hdc.cs.arizona.edu/~mwli/graph-drawing/>.
 182

183 **4 Properties and Measures**

184 In this section we specify the aesthetic goals, definitions, quality measures and
 185 loss functions for each of the 9 graph drawing properties we optimized: stress,
 186 vertex resolution, edge uniformity, neighborhood preservation, crossing angle,
 187 aspect ratio, total angular resolution, Gabriel graph property, and crossing num-
 188 ber. In the following discussion, since only one (arbitrary) graph is considered,
 189 we omit the subscript G in our definitions of loss function $L_{Q,G}$ and write L_Q
 190 for short. Other standard graph notation is summarized in Table 1.

Notation	Description
G	Graph
V	The set of nodes in G , indexed by i, j or k
E	The set of edges in G , indexed by a pair of nodes (i, j) in V
$n = V $	Number of nodes in G
$ E $	Number of edges in G
$Adj_{n \times n}$ and $A_{i,j}$	Adjacency matrix of G and its (i, j) -th entry
$D_{n \times n}$ and d_{ij}	Graph-theoretic distances between pairs of nodes and the (i, j) -th entry
$X_{n \times 2}$	2D-coordinates of nodes in the drawing
$\ X_i - X_j\ $	The Euclidean distance between nodes i and j in the drawing
θ_i	i^{th} crossing angle
φ_{ijk}	Angle between incident edges (i, j) and (j, k)

191 **Table 1.** Graph notation used in this paper.192 **4.1 Stress**

193 We use stress minimization to draw a graph such that the Euclidean distance be-
 194 tween pairs of nodes is proportional to their graph theoretic distance. Following
 195 the ordinary definition of stress [24], we minimize

$$L_{ST} = \sum_{i < j} w_{ij} (\|X_i - X_j\|_2 - d_{ij})^2 \quad (1)$$

196 Where d_{ij} is the graph-theoretical distance between nodes i and j , X_i and X_j
 197 are the 2D coordinates of nodes i and j in the layout. The normalization factor,
 198 $w_{ij} = d_{ij}^{-2}$, balances the influence of short and long distances: the longer the
 199 graph theoretic distance, the more tolerance we give to the discrepancy between
 200 two distances. When comparing two drawings of the same graph with respect to
 201 stress, a smaller value (lower bounded by 0) corresponds to a better drawing.

202 4.2 Ideal Edge Length

203 When given a set of ideal edge lengths $\{l_{ij} : (i, j) \in E\}$ we minimize the average
 204 deviation from the ideal lengths:

$$L_{IL} = \sqrt{\frac{1}{|E|} \sum_{(i,j) \in E} \left(\frac{\|X_i - X_j\| - l_{ij}}{l_{ij}} \right)^2} \quad (2)$$

205 For unweighted graphs, by default we take the average edge length in the current
 206 drawing as the ideal edge length for all edges. $l_{ij} = l_{avg} = \frac{1}{|E|} \sum_{(i,j) \in E} \|X_i -$
 207 $X_j\|$ for all $(i, j) \in E$. The quality measure $Q_{IL} = L_{IL}$ is lower bounded by
 208 0 and a lower score yields a better layout.

209 4.3 Neighborhood Preservation

210 Neighborhood preservation aims to keep adjacent nodes close to each other in
 211 the layout. Similar to Krueger et al. [25], the idea is to have the k -nearest (Eu-
 212 clidean) neighbors (k-NN) of node i in the drawing to align with the k near-
 213 est nodes (in terms of graph distance from i). A natural quality measure for
 214 the alignment is the Jaccard index between the two pieces of information. Let,
 215 $Q_{NP} = JaccardIndex(K, Adj) = \frac{|\{(i,j):K_{ij}=1 \text{ and } A_{ij}=1\}|}{|\{(i,j):K_{ij}=1 \text{ or } A_{ij}=1\}|}$, where Adj denotes the
 216 adjacency matrix and the i -th row in K denotes the k -nearest neighborhood in-
 217 formation of i : $K_{ij} = 1$ if j is one of the k -nearest neighbors of i and $K_{ij} = 0$
 218 otherwise.

219 To express the Jaccard index as a differentiable minimization problem, first,
 220 we express the neighborhood information in the drawing as a smooth function of
 221 node positions X_i and store it in a matrix \hat{K} . In \hat{K} , a positive entry $\hat{K}_{i,j}$ means
 222 node j is one of the k -nearest neighbors of i , otherwise the entry is negative. Next,
 223 we take a differentiable surrogate function of the Jaccard index, the Lovász hinge
 224 loss (LHL) [5], to make the Jaccard loss optimizable via gradient descent. We
 225 minimize

$$L_{NP} = LHL(\hat{K}, Adj) \quad (3)$$

226 where LHL is given by Berman et al. [5], \hat{K} denotes the k -nearest neighbor
 227 prediction:

$$\hat{K}_{i,j} = \begin{cases} -(\|X_i - X_j\| - \frac{d_{i,\pi_k} + d_{i,\pi_{k+1}}}{2}) & \text{if } i \neq j \\ 0 & \text{if } i = j \end{cases} \quad (4)$$

228 where d_{i,π_k} is the Euclidean distance between node i and its k^{th} nearest neighbor
 229 and Adj denotes the adjacency matrix. Note that $\hat{K}_{i,j}$ is positive if j is a k-NN
 230 of i , otherwise it is negative, as is required by LHL [5].

231 **4.4 Crossing Number**

232 Reducing the number of edge crossings is one of the classic optimization goals in
 233 graph drawing, known to affect readability [28]. Following Shabbeer et al. [31],
 234 we employ an expectation-maximization (EM)-like algorithm to minimize the
 235 number of crossings. Two edges do not cross if and only if there exists a line
 236 that separate their extreme points. With this in mind, we want to separate
 237 every pair of edges (the M step) and use the decision boundaries to guide the
 238 movement of nodes in the drawing (the E step). Formally, given any two edges
 239 $e_1 = (i, j), e_2 = (k, l)$ that do not share any nodes (i.e., i, j, k and l are all
 240 distinct), they do not intersect in a drawing (where nodes are drawn at $X_i =$
 241 (x_i, y_i) , a row vector) if and only if there exists a decision boundary $w = w_{(e_1, e_2)}$
 242 (a 2-by-1 column vector) together with a bias $b = b_{(e_1, e_2)}$ (a scalar) such that:
 243 $L_{CN, (e_1, e_2)} = \sum_{\alpha=i, j, k \text{ or } l} ReLU(1 - t_\alpha \cdot (X_\alpha w + b)) = 0$.

244 Here we use (e_1, e_2) to denote the subgraph of G which only has two edges
 245 e_1 and e_2 , $t_i = t_j = 1$ and $t_k = t_l = -1$. The loss reaches its minimum at 0 when
 246 the SVM classifier $f_{w, b} : x \mapsto xw + b$ predicts node i and j to be greater than 1
 247 and node k and l to be less than -1 . The total loss for the crossing number is
 248 therefore the sum over all possible pairs of edges. Similar to (soft) margin SVM,
 249 we add a term $|w_{(e_1, e_2)}|^2$ to maximize the margin of the decision boundary:
 250 $L_{CN} = \sum_{\substack{e_1=(i,j), e_2=(k,l) \in E \\ i, j, k \text{ and } l \text{ all distinct}}} L_{CN, (e_1, e_2)} + |w_{(e_1, e_2)}|^2$. For the E and M steps, we

251 used the same loss function L_{CN} to update the boundaries $w_{(e_1, e_2)}, b_{(e_1, e_2)}$ and
 252 node positions X :

$$w^{(new)} = w - \epsilon \nabla_w L_{CN} \quad (\text{M step 1})$$

$$b^{(new)} = b - \epsilon \nabla_b L_{CN} \quad (\text{M step 2})$$

$$X^{(new)} = X - \epsilon \nabla_X L_{CN}(X; w^{(new)}, b^{(new)}) \quad (\text{E step})$$

253 To evaluate the quality we simply count the number of crossings.

254 **4.5 Crossing Angle Maximization**

255 When edge crossings are unavoidable, the graph drawing can still be easier to
 256 read when edges cross at angles close to 90 degrees [35]. Heuristics such as those
 257 by Demel et al. [10] and Bekos et al. [4] have been proposed and have been
 258 successful in graph drawing challenges [11]. We use an approach similar to the
 259 force-directed algorithm given by Eades et al. [18] and minimize the squared
 260 cosine of crossing angles: $L_{CAM} = \sum_{\substack{\text{all crossed edge pairs} \\ (i,j), (k,l) \in E}} \left(\frac{\langle X_i - X_j, X_k - X_l \rangle}{|X_i - X_j| \cdot |X_k - X_l|} \right)^2$. We
 261 evaluate quality by measuring the worst (normalized) absolute discrepancy be-
 262 tween each crossing angle θ and the target crossing angle (i.e. 90 degrees):
 263 $Q_{CAM} = \max_\theta |\theta - \frac{\pi}{2}| / \frac{\pi}{2}$.

264 4.6 Aspect Ratio

265 Good use of drawing area is often measured by the aspect ratio [14] of the
 266 bounding box of the drawing, with 1 : 1 as the optimum. We consider multiple
 267 rotations of the current drawing and optimize their bounding boxes simultane-
 268 ously. Let $AR = \min_{\theta} \frac{\min(w_{\theta}, h_{\theta})}{\max(w_{\theta}, h_{\theta})}$, where w_{θ} and h_{θ} denote the width and height
 269 of the bounding box when the drawing is rotated by θ degrees. A naive approach
 270 to optimize aspect ratio, which scales the x and y coordinates of the drawing by
 271 certain factors, may worsen other criteria we wish to optimize and is therefore
 272 not suitable for our purposes. To make aspect ratio differentiable and compatible
 273 with other objectives, we approximate aspect ratio based on 4 (soft) boundaries
 274 (top, bottom, left and right) of the drawing. Next, we turn this approximation
 275 and the target (1 : 1) into a loss function using cross entropy loss. We minimize

$$L_{AR} = \sum_{\theta \in \{\frac{2\pi k}{N}, \text{ for } k=0, \dots, (N-1)\}} \text{crossEntropy}\left(\left[\frac{w_{\theta}}{w_{\theta} + h_{\theta}}, \frac{h_{\theta}}{w_{\theta} + h_{\theta}}\right], [0.5, 0.5]\right) \quad (5)$$

276 where N is the number of rotations sampled (e.g., $N = 7$), and w_{θ} , h_{θ} are the
 277 (approximate) width and height of the bounding box when rotating the drawing
 278 around its center by an angle θ . For any given θ -rotated drawing, w_{θ} is defined
 279 to be the difference between the current (soft) right and left boundaries, $w_{\theta} =$
 280 $\text{right} - \text{left} = \langle \text{softmax}(x_{\theta}), x_{\theta} \rangle - \langle \text{softmax}(-x_{\theta}), x_{\theta} \rangle$, where x_{θ} is a collection
 281 of the x coordinates of all nodes in the θ -rotated drawing, and softmax returns a
 282 vector of weights ($\dots w_k, \dots$) given by $\text{softmax}(x) = (\dots w_k, \dots) = \frac{e^{x_k}}{\sum_i e^{x_i}}$. Note
 283 that the approximate right boundary is a weighted sum of the x coordinates
 284 of all nodes and it is designed to be close to the x coordinate of the right-
 285 most node, while keeping other nodes involved. Optimizing aspect ratio with
 286 the softened boundaries will stretch all nodes instead of moving the extreme
 287 points. Similarly, $h_{\theta} = \text{top} - \text{bottom} = \langle \text{softmax}(y_{\theta}), y_{\theta} \rangle - \langle \text{softmax}(-y_{\theta}), y_{\theta} \rangle$
 288 Finally, we evaluate the drawing quality by measuring the worst aspect ratio
 289 on a finite set of rotations. The quality score ranges from 0 to 1 (where 1 is
 290 optimal): $Q_{AR} = \min_{\theta \in \{\frac{2\pi k}{N}, \text{ for } k=0, \dots, (N-1)\}} \frac{\min(w_{\theta}, h_{\theta})}{\max(w_{\theta}, h_{\theta})}$

291 4.7 Angular Resolution

292 Distributing edges adjacent to a node makes it easier to perceive the informa-
 293 tion presented in a node-link diagram [23]. Angular resolution [3], defined as the
 294 minimum angle between incident edges, is one way to quantify this goal. For-
 295 mally, $ANR = \min_{j \in V} \min_{(i,j), (j,k) \in E} \varphi_{ijk}$, where φ_{ijk} is the angle formed by
 296 between edges (i, j) and (j, k) . Note that for any given graph, an upper bound
 297 of this quantity is $\frac{2\pi}{d_{max}}$ where d_{max} is the maximum degree of nodes in the
 298 graph. Therefore in the evaluation, we will use this upper bound to normalize
 299 our quality measure to $[0, 1]$, i.e. $Q_{ANR} = \frac{ANR}{2\pi/d_{max}}$. To achieve a better drawing

300 quality via gradient descent, we define the angular energy of an angle φ to be
 301 $e^{-s \cdot \varphi}$, where s is a constant controlling the sensitivity of angular energy with
 302 respect to the angle (by default $s = 1$), and minimize the total angular energy
 303 over all incident edges:

$$L_{ANR} = \sum_{(i,j),(j,k) \in E} e^{-s \cdot \varphi_{ijk}} \quad (6)$$

304 4.8 Vertex Resolution

305 Good vertex resolution is associated with the ability to distinguish different
 306 vertices by preventing nodes from occluding each other. Vertex resolution is
 307 typically defined as the minimum Euclidean distance between two vertices in
 308 the drawing [9,30]. However, in order to align with the units in other objectives
 309 such as stress, we normalize the minimum Euclidean distance with respect to a
 310 reference value. Hence we define the vertex resolution to be the ratio between
 311 the shortest and longest distances between pairs of nodes in the drawing, $VR =$
 312 $\frac{\min_{i \neq j} \|X_i - X_j\|}{d_{max}}$, where $d_{max} = \max_{k,l} \|X_k - X_l\|$. To achieve a certain target
 313 resolution $r \in [0, 1]$ by minimizing a loss function, we minimize

$$L_{VR} = \sum_{i,j \in V, i \neq j} ReLU(1 - \frac{\|X_i - X_j\|}{r \cdot d_{max}})^2 \quad (7)$$

314 In practice, we set the target resolution to be $r = \frac{1}{\sqrt{|V|}}$, where $|V|$ is the number
 315 of vertices in the graph. In this way, an optimal drawing will distribute nodes
 316 uniformly in the drawing area. In the evaluation, we report, as a quality measure,
 317 the ratio between the actual and target resolution and cap its value between 0
 318 (worst) and 1 (best).

$$Q_{VR} = \min(1.0, \frac{\min_{i,j} \|X_i - X_j\|}{r \cdot d_{max}}) \quad (8)$$

319 4.9 Gabriel Graph Property

320 A graph is a Gabriel graph if it can be drawn in such a way that any disk
 321 formed by using an edge in the graph as its diameter contains no other nodes.
 322 Not all graphs are Gabriel graphs, but drawing a graph so that as many of
 323 these edge-based disks are empty of other nodes has been associated with good
 324 readability [17]. This property can be enforced by a repulsive force around the
 325 midpoints of edges. Formally, we establish a repulsive field with radius r_{ij} equal
 326 to half of the edge length, around the midpoint c_{ij} of each edge $(i, j) \in E$, and
 327 we minimize the total potential energy:

$$L_{GA} = \sum_{\substack{(i,j) \in E, \\ k \in V \setminus \{i,j\}}} \text{ReLU}(r_{ij} - |X_k - c_{ij}|)^2 \quad (9)$$

328 where $c_{ij} = \frac{X_i + X_j}{2}$ and $r_{ij} = \frac{|X_i - X_j|}{2}$. We use the (normalized) minimum dis-
 329 tance from nodes to centers to characterize the quality of a drawing with respect
 330 to Gabriel graph property: $Q_{GA} = \min_{(i,j) \in E, k \in V} \frac{|X_k - c_{ij}|}{r_{ij}}$.

331 5 Experimental Evaluation

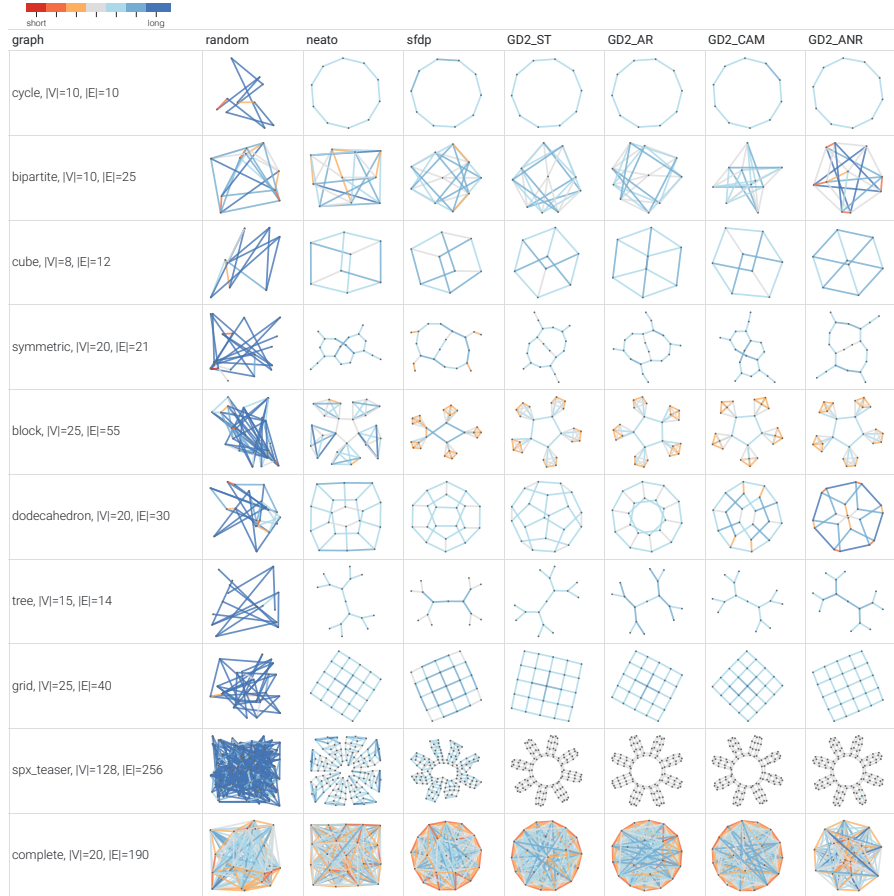
332 In this section, we describe the experiment we conducted on 10 graphs to assess
 333 the effectiveness and limitations of our approach. The graphs used are depicted
 334 in Figure 3 along with information about each graph. The graphs have been
 335 chosen to represent a variety of graph classes such as trees, cycles, grids, bipartite
 336 graphs, cubic graphs, and symmetric graphs.

337 In our experiment we compare $(GD)^2$ with neato [19] and sfdp [19], which
 338 are classical implementations of a stress-minimization layout and scalable force-
 339 directed layout. In particular, we focus on 9 readability criteria: stress (ST), ver-
 340 tex resolution (VR), ideal edge lengths (IL), neighbor preservation (NP), crossing
 341 angle (CA), angular resolution (ANR), aspect ratio (AR), Gabriel graph properties
 342 (GG), and crossings (CR). We provide the values of the nine criteria correspond-
 343 ing to the 10 graphs for the layouts computed by by neato, sfdp, random, and 3
 344 runs of $(GD)^2$ initialized with neato, sfdp, and random layouts in Table 2. Bold
 345 values are the best. Green cells show an improvement, yellow cells show a tie,
 346 with respect to the initial values.

352 In this experiment, we focused on optimizing a single metric. In some applica-
 353 tions, it is desirable to optimize multiple criteria. We can use a similar technique
 354 i.e., take a weighted sum of the metrics and optimize the sum of scores. In the
 355 prototype (<http://hdc.cs.arizona.edu/~mwli/graph-drawing/>), there is a
 356 slider for each criterion, making it possible to combine different criteria.

357 6 Limitations

358 Although $(GD)^2$ is a flexible framework that can optimize a wide range of crite-
 359 ria, it cannot handle the class of constraints where the node coordinates are re-
 360 lated by some inequalities, i.e., the framework does not support hard constraints.
 361 Similarly, this framework does not naturally support shape-based drawing con-
 362 straints such as those in [15, 16, 34]. $(GD)^2$ takes under a minute for the small
 363 graphs considered in this paper. We have not experimented with larger graphs
 364 as the implementation has not been optimized for speed.



347 **Fig. 3.** Drawings from different algorithms: neato, sfdp and $(GD)^2$ with stress
 348 (ST), aspect ratio (AR), crossing angle maximization (CAM) and angular resolution
 349 (ANR) optimization on a set of 10 graphs. Edge color is determined by the
 350 discrepancy between actual and ideal edge length (here all ideal edge lengths are
 351 1); informally, short edges are red and long edges are blue.

365 7 Conclusions and Future Work

366 We introduced the graph drawing framework $(GD)^2$ and showed how this ap-
 367 proach can be used to optimize different graph drawing criteria and combinations
 368 thereof. The framework is flexible and natural directions for future work include
 369 adding further drawing criteria and better ways to combine them. To compute
 370 the layout of large graphs, a multi-level algorithmic model might be needed.

Crossings						
	neato	sdfp	rnd	$(GD)_n^2$	$(GD)_s^2$	$(GD)_r^2$
dodec.	6.0	6.0	79.0	6.0	6.0	10.0
cycle	0.0	0.0	11.0	0.0	0.0	0.0
tree	0.0	0.0	31.0	0.0	0.0	0.0
block	23.0	16.0	297.0	23.0	16.0	25.0
compl.	3454	3571	3572	3454	3571	3572
cube	2.0	2.0	18.0	2.0	2.0	2.0
symme.	1.0	0.0	77.0	1.0	0.0	0.0
bipar.	40.0	52.0	40.0	40.0	40.0	40.0
grid	0.0	0.0	190.0	0.0	0.0	0.0
spx t.	73.0	71.0	7254.0	73.0	71.0	76.0

Ideal edge length						
	neato	sdfp	rnd	$(GD)_n^2$	$(GD)_s^2$	$(GD)_r^2$
dodec.	0.14	0.15	0.53	0.1	0.15	0.08
cycle	0.0	0.0	0.42	0.0	0.0	0.0
tree	0.03	0.13	0.31	0.03	0.04	0.09
block	0.31	0.43	0.5	0.25	0.33	0.31
compl.	0.42	0.41	0.45	0.41	0.41	0.41
cube	0.08	0.12	0.29	0.03	0.0	0.12
symme.	0.08	0.19	0.46	0.07	0.05	0.04
bipar.	0.31	0.26	0.44	0.16	0.13	0.1
grid	0.01	0.09	0.41	0.0	0.0	0.01
spx t.	0.4	0.32	0.45	0.3	0.2	0.32

Stress						
	neato	sdfp	rnd	$(GD)_n^2$	$(GD)_s^2$	$(GD)_r^2$
dodec.	21.4	17.58	111.05	17.45	17.58	17.6
cycle	0.77	0.77	30.24	0.77	0.77	0.77
tree	2.11	2.7	98.49	2.11	2.62	5.5
block	26.79	28.22	203.31	12.72	23.71	11.2
compl.	33.54	31.58	37.87	31.53	31.49	31.47
cube	2.75	2.71	11.69	2.66	2.69	2.65
symme.	9.88	5.38	180.48	9.88	3.36	3.97
bipar.	9.25	8.5	12.48	8.52	8.5	9.6
grid	6.77	7.38	221.66	6.77	6.78	6.77
spx t.	674.8	418.4	9794	227.1	235.3	227.2

Angular resolution						
	neato	sdfp	rnd	$(GD)_n^2$	$(GD)_s^2$	$(GD)_r^2$
dodec.	0.39	0.39	0.01	0.6	0.39	0.6
cycle	0.8	0.8	0.05	0.8	0.8	0.8
tree	0.61	0.56	0.04	0.78	0.83	0.88
block	0.05	0.01	0.0	0.36	0.02	0.29
compl.	0.0	0.01	0.0	0.0	0.01	0.0
cube	0.28	0.3	0.01	0.46	0.44	0.4
symme.	0.66	0.6	0.03	0.68	0.76	0.77
bipar.	0.01	0.03	0.01	0.02	0.04	0.11
grid	0.52	0.54	0.0	0.52	0.54	0.52
spx t.	0.02	0.0	0.0	0.03	0.0	0.0

Neighbor preservation						
	neato	sdfp	rnd	$(GD)_n^2$	$(GD)_s^2$	$(GD)_r^2$
dodec.	0.32	0.3	0.1	0.5	0.3	0.5
cycle	1.0	1.0	0.08	1.0	1.0	1.0
tree	1.0	1.0	0.02	1.0	1.0	1.0
block	0.57	0.93	0.12	0.83	0.93	1.0
compl.	1.0	1.0	1.0	1.0	1.0	1.0
cube	0.5	0.5	0.12	0.5	0.5	0.5
symme.	0.75	0.95	0.05	0.75	1.0	1.0
bipar.	0.47	0.47	0.43	0.47	0.47	0.43
grid	1.0	1.0	0.05	1.0	1.0	1.0
spx t.	0.36	0.44	0.03	0.49	0.46	0.53

Gabriel graph property						
	neato	sdfp	rnd	$(GD)_n^2$	$(GD)_s^2$	$(GD)_r^2$
dodec.	0.16	0.64	0.07	0.32	0.64	0.32
cycle	1.0	1.0	0.29	1.0	1.0	1.0
tree	1.0	1.0	0.05	1.0	1.0	1.0
block	0.16	0.03	0.04	0.57	0.14	0.59
compl.	0.0	0.01	0.02	0.04	0.01	0.07
cube	0.43	0.51	0.01	0.75	0.8	0.71
symme.	0.54	1.0	0.15	0.7	1.0	1.0
bipar.	0.08	0.11	0.25	0.48	0.64	0.74
grid	1.0	1.0	0.03	1.0	1.0	1.0
spx t.	0.04	0.0	0.02	0.06	0.08	0.08

Vertex resolution						
	neato	sdfp	rnd	$(GD)_n^2$	$(GD)_s^2$	$(GD)_r^2$
dodec.	0.52	0.54	0.07	0.7	0.81	0.68
cycle	0.98	0.98	0.32	0.98	0.98	0.98
tree	0.68	0.57	0.23	0.69	0.68	0.68
block	0.66	0.38	0.1	0.72	0.59	0.51
compl.	0.8	1.0	0.18	0.84	1.0	0.91
cube	0.66	0.82	0.11	0.66	0.82	0.67
symme.	0.35	0.43	0.06	0.38	0.51	0.6
bipar.	0.83	0.87	0.21	0.83	0.87	0.35
grid	0.87	0.8	0.08	0.88	0.88	0.88
spx t.	0.47	0.48	0.05	0.47	0.48	0.32

Aspect ratio						
	neato	sdfp	rnd	$(GD)_n^2$	$(GD)_s^2$	$(GD)_r^2$
dodec.	0.92	0.91	0.88	0.96	0.96	0.96
cycle	0.96	0.95	0.67	0.96	0.95	0.96
tree	0.73	0.67	0.88	0.86	0.76	0.88
block	0.9	0.74	0.7	0.96	0.9	0.96
compl.	0.89	0.97	0.91	0.98	0.98	0.98
cube	0.76	0.79	0.57	0.87	0.79	0.88
symme.	0.58	0.67	0.89	0.6	0.67	0.89
bipar.	0.82	0.9	0.91	0.82	0.9	0.91
grid	1.0	1.0	0.82	1.0	1.0	1.0
spx t.	0.98	0.86	0.88	0.99	0.99	0.99

Crossing angle						
	neato	sdfp	rnd	$(GD)_n^2$	$(GD)_s^2$	$(GD)_r^2$
dodec.	0.06	0.12	0.24	0.06	0.09	0.15
cycle	0.0	0.0	0.19	0.0	0.0	0.0
tree	0.0	0.0	0.23	0.0	0.0	0.0
block	0.11	0.1	0.24	0.05	0.06	0.09
compl.	0.25	0.24	0.24	0.24	0.24	0.24
cube	0.03	0.03	0.21	0.03	0.03	0.04
symme.	0.03	0.0	0.24	0.03	0.0	0.0
bipar.	0.16	0.17	0.23	0.16	0.17	0.19
grid	0.0	0.0	0.23	0.0	0.0	0.0
spx t.	0.16	0.22	0.25	0.16	0.15	0.21

371 **Table 2.** The values of the nine criteria corresponding to the 10 graphs for the
 372 layouts computed by neato, sdfp, random, and 3 runs of $(GD)^2$ initialized with
 373 neato, sdfp, and random layouts. Bold values are the best. Green cells show an
 374 improvement, yellow cells show a tie, with respect to the initial values.

375 **References**

- 376 1. Abadi, M., Barham, P., Chen, J., Chen, Z., Davis, A., Dean, J., Devin, M., Ghe-
377 mawat, S., Irving, G., Isard, M., et al.: Tensorflow: A system for large-scale machine
378 learning. In: 12th USENIX Symposium on Operating Systems Design and Imple-
379 mentation (OSDI'16). pp. 265–283 (2016)
- 380 2. Ábrego, B.M., Fernández-Merchant, S., Salazar, G.: The rectilinear crossing num-
381 ber of k_n : Closing in (or are we?). *Thirty Essays on Geometric Graph Theory*
382 (2012)
- 383 3. Argyriou, E.N., Bekos, M.A., Symvonis, A.: Maximizing the total resolution of
384 graphs. In: *Proceedings of the 18th International Conference on Graph Drawing*.
385 pp. 62–67. Springer (2011)
- 386 4. Bekos, M.A., Förster, H., Geckeler, C., Holländer, L., Kaufmann, M., Spallek,
387 A.M., Splett, J.: A heuristic approach towards drawings of graphs with high cross-
388 ing resolution. In: *Proceedings of the 26th International Symposium on Graph*
389 *Drawing and Network Visualization*. pp. 271–285. Springer (2018)
- 390 5. Berman, M., Rannen Triki, A., Blaschko, M.B.: The lovász-softmax loss: a tractable
391 surrogate for the optimization of the intersection-over-union measure in neural
392 networks. In: *Proceedings of the IEEE Conference on Computer Vision and Pattern*
393 *Recognition*. pp. 4413–4421 (2018)
- 394 6. Bostock, M., Ogievetsky, V., Heer, J.: D3: Data-driven documents. *IEEE transac-*
395 *tions on visualization and computer graphics* **17**(12), 2301–2309 (2011)
- 396 7. Buchheim, C., Chimani, M., Gutwenger, C., Jünger, M., Mutzel, P.: Crossings and
397 planarization. *Handbook of Graph Drawing and Visualization* pp. 43–85 (2013)
- 398 8. Chen, K.T., Dwyer, T., Marriott, K., Bach, B.: Doughnets: Visualising networks
399 using torus wrapping. In: *Proceedings of the 2020 CHI Conference on Human*
400 *Factors in Computing Systems*. pp. 1–11 (2020)
- 401 9. Chrobak, M., Goodrich, M.T., Tamassia, R.: Convex drawings of graphs in two and
402 three dimensions. In: *Proceedings of the 12th annual symposium on Computational*
403 *geometry*. pp. 319–328 (1996)
- 404 10. Demel, A., Dürrschnabel, D., Mchedlidze, T., Radermacher, M., Wulf, L.: A greedy
405 heuristic for crossing-angle maximization. In: *Proceedings of the 26th International*
406 *Symposium on Graph Drawing and Network Visualization*. pp. 286–299. Springer
407 (2018)
- 408 11. Devanny, W., Kindermann, P., Löffler, M., Rutter, I.: Graph drawing contest re-
409 port. In: *Proceedings of the 25th International Symposium on Graph Drawing and*
410 *Network Visualization*. pp. 575–582. Springer (2017)
- 411 12. Devkota, S., Ahmed, R., De Luca, F., Isaacs, K.E., Kobourov, S.: Stress-plus-x
412 (spx) graph layout. In: *Proceedings of the 27th International Symposium on Graph*
413 *Drawing and Network Visualization*. pp. 291–304. Springer (2019)
- 414 13. Didimo, W., Liotta, G.: The crossing-angle resolution in graph drawing. *Thirty*
415 *Essays on Geometric Graph Theory* (2014)
- 416 14. Duncan, C.A., Goodrich, M.T., Kobourov, S.G.: Balanced aspect ratio trees and
417 their use for drawing very large graphs. In: *Proceedings of the 6th International*
418 *Symposium on Graph Drawing*. pp. 111–124. Springer (1998)
- 419 15. Dwyer, T.: Scalable, versatile and simple constrained graph layout. *Comput.*
420 *Graph. Forum* **28**, 991–998 (2009)
- 421 16. Dwyer, T., Koren, Y., Marriott, K.: Ipsep-cola: An incremental procedure for sep-
422 aration constraint layout of graphs. *IEEE transactions on visualization and com-*
423 *puter graphics* **12**, 821–8 (2006)

- 424 17. Eades, P., Hong, S.H., Klein, K., Nguyen, A.: Shape-based quality metrics for large
425 graph visualization. In: Proceedings of the 23rd International Conference on Graph
426 Drawing and Network Visualization. pp. 502–514. Springer (2015)
- 427 18. Eades, P., Huang, W., Hong, S.H.: A force-directed method for large crossing angle
428 graph drawing. arXiv preprint arXiv:1012.4559 (2010)
- 429 19. Ellson, J., Gansner, E., Koutsofios, L., North, S.C., Woodhull, G.: Graphviz—open
430 source graph drawing tools. In: Proceedings of the 9th International Symposium
431 on Graph Drawing. pp. 483–484. Springer (2001)
- 432 20. Gansner, E.R., Koren, Y., North, S.: Graph drawing by stress majorization. In:
433 International Symposium on Graph Drawing. pp. 239–250. Springer (2004)
- 434 21. Griewank, A., Walther, A.: Evaluating derivatives: principles and techniques of
435 algorithmic differentiation, vol. 105. SIAM (2008)
- 436 22. Huang, W., Eades, P., Hong, S.H.: Larger crossing angles make graphs easier to
437 read. *Journal of Visual Languages & Computing* **25**(4), 452–465 (2014)
- 438 23. Huang, W., Eades, P., Hong, S.H., Lin, C.C.: Improving multiple aesthetics pro-
439 duces better graph drawings. *Journal of Visual Languages & Computing* **24**(4),
440 262 – 272 (2013)
- 441 24. Kamada, T., Kawai, S.: An algorithm for drawing general undirected graphs. *In-*
442 *formation Processing Letters* **31**(1), 7 – 15 (1989)
- 443 25. Krueger, J.F., Rauber, P.E., Martins, R.M., Kerren, A., Kobourov, S., Telea, A.C.:
444 Graph layouts by t-sne. *Comput. Graph. Forum* **36**(3), 283–294 (2017)
- 445 26. Kruskal, J.B.: Multidimensional scaling by optimizing goodness of fit to a non-
446 metric hypothesis. *Psychometrika* **29**(1), 1–27 (1964)
- 447 27. Paszke, A., Gross, S., Massa, F., Lerer, A., Bradbury, J., Chanan, G., Killeen,
448 T., Lin, Z., Gimelshein, N., Antiga, L., et al.: Pytorch: An imperative style, high-
449 performance deep learning library. In: *Advances in Neural Information Processing*
450 *Systems*. pp. 8024–8035 (2019)
- 451 28. Purchase, H.: Which aesthetic has the greatest effect on human understanding? In:
452 *Proceedings of the 5th International Symposium on Graph Drawing*. pp. 248–261.
453 Springer (1997)
- 454 29. Radermacher, M., Reichard, K., Rutter, I., Wagner, D.: A geometric heuristic for
455 rectilinear crossing minimization. In: *The 20th Workshop on Algorithm Engineer-*
456 *ing and Experiments*. p. 129–138 (2018)
- 457 30. Schulz, A.: Drawing 3-polytopes with good vertex resolution. *J. Graph Algorithms*
458 *Appl.* **15**(1), 33–52 (2011)
- 459 31. Shabbeer, A., Ozcaglar, C., Gonzalez, M., Bennett, K.P.: Optimal embedding of
460 heterogeneous graph data with edge crossing constraints. In: *NIPS Workshop on*
461 *Challenges of Data Visualization* (2010)
- 462 32. Shepard, R.N.: The analysis of proximities: multidimensional scaling with an un-
463 known distance function. *Psychometrika* **27**(2), 125–140 (1962)
- 464 33. Smilkov, D., Thorat, N., Assogba, Y., Nicholson, C., Kreeger, N., Yu, P., Cai,
465 S., Nielsen, E., Soegel, D., Bileschi, S., Terry, M., Yuan, A., Zhang, K., Gupta,
466 S., Sirajuddin, S., Sculley, D., Monga, R., Corrado, G., Viegas, F., Wattenberg,
467 M.M.: Tensorflow.js: Machine learning for the web and beyond. In: *Proceedings of*
468 *Machine Learning and Systems 2019*, pp. 309–321 (2019)
- 469 34. Wang, Y., Wang, Y., Sun, Y., Zhu, L., Lu, K., Fu, C.W., Sedlmair, M., Deussen,
470 O., Chen, B.: Revisiting stress majorization as a unified framework for interactive
471 constrained graph visualization. *IEEE transactions on visualization and computer*
472 *graphics* **24**(1), 489–499 (2017)
- 473 35. Ware, C., Purchase, H., Colpoys, L., McGill, M.: Cognitive measurements of graph
474 aesthetics. *Information visualization* **1**(2), 103–110 (2002)

- 475 36. Zheng, J.X., Pawar, S., Goodman, D.F.: Graph drawing by stochastic gradient
476 descent. *IEEE transactions on visualization and computer graphics* **25**(9), 2738–
477 2748 (2018)

478 **8 Appendix**

480 The following table summarizes the objective functions used to optimize the nine drawing criteria via different optimization methods.

Property	Gradient Descent	Subgradient Descent	Stochastic Gradient Descent
Stress	$\sum_{i < j} w_{ij}(X_i - X_j _2 - d_{ij})^2$	$\sum_{i < j} w_{ij}(X_i - X_j _2 - d_{ij})^2$	$w_{ij}(X_i - X_j _2 - d_{ij})^2$ for a random pair of nodes $i, j \in V$
Ideal Edge Length (Eq. 2)	$\sqrt{\frac{1}{ E } \sum_{(i,j) \in E} \left(\frac{\ X_i - X_j\ - l_{ij}}{l_{ij}}\right)^2}$	$\frac{1}{ E } \sum_{(i,j) \in E} \left \frac{\ X_i - X_j\ - l_{ij}}{l_{ij}}\right $	$\left \frac{\ X_i - X_j\ - l_{ij}}{l_{ij}}\right $ for a random edge $(i, j) \in E$
Crossing Angle	$\sum_i \cos(\theta_i)^2$	$\sum_i \cos(\theta_i) $	$ \cos(\theta_i) $ for a random crossing i
Neighborhood Preservation	Lovász softmax [5] between neighborhood prediction (Eq.4) and adjacency matrix Adj	Lovász hinge [5] between neighborhood prediction (Eq.4) and adjacency matrix Adj	Lovász softmax or hinge [5] on a random node. (i.e. Jaccard loss between a random row of K in Eq. 4 and the corresponding row in the adjacency matrix Adj)
Crossing Number	Shabbeer et al. [31]	Shabbeer et al. [31]	Shabbeer et al. [31]
Angular Resolution	$\sum_{(i,j),(j,k) \in E} e^{-\varphi_{ijk}}$	$\sum_{v \in E} e^{-\varphi_{ijk}}$	$e^{-\varphi_{ijk}}$ for random $(i, j), (j, k) \in E$
Vertex Resolution (Eq. 7)	$\sum_{i,j \in V, i \neq j} ReLU\left(1 - \frac{\ X_i - X_j\ }{d_{max} \cdot r}\right)^2$	$\sum_{i,j \in V, i \neq j} ReLU\left(1 - \frac{\ X_i - X_j\ }{d_{max} \cdot r}\right)$	$ReLU\left(1 - \frac{\ X_i - X_j\ }{d_{max} \cdot r}\right)$ for random $i, j \in V, i \neq j$
Gabriel Graph (Eq. 9)	$\sum_{(i,j) \in E, k \in V \setminus \{i,j\}} ReLU(r_{ij} - \ X_k - c_{ij}\)^2$	$\sum_{(i,j) \in E, k \in V \setminus \{i,j\}} ReLU(r_{ij} - \ X_k - c_{ij}\)$	$ReLU(r_{ij} - \ X_k - c_{ij}\)$ for random $(i, j) \in E$ and $k \in V \setminus \{i, j\}$
Aspect Ratio	Eq. 5	Eq. 5	Eq. 5

479 **Table 3.** Summary of the objective functions via different optimization methods.